A Learning-Based Approach for Traffic State Reconstruction from Limited Data

Nail Baloul, Amaury Hayat, Thibault Liard, Pierre Lissy

SMAI 2025, Carcans Maubuisson

June, 3rd 2025

Outline

Table of Contents

Motivation

Traffic jam in Beijing

- Traffic congestion is a main contributor of air pollution and excessive travel time
  $\Rightarrow$ impacts urban mobility and environmental quality

Motivation

Traffic jam in Beijing

- Traffic congestion is a main contributor of air pollution and excessive travel time
  $\Rightarrow$ impacts urban mobility and environmental quality
- Traffic management relies on **control** schemes to address perturbed traffic conditions
- Most existing control techniques require complete and accurate knowledge of state
- In practice, full information is rarely available due to limited and noisy measurements

Motivation

Traffic jam in Beijing

- Traffic congestion is a main contributor of air pollution and excessive travel time
  $\Rightarrow$ impacts urban mobility and environmental quality
- Traffic management relies on **control** schemes to address perturbed traffic conditions
- Most existing control techniques require complete and accurate knowledge of state
- In practice, full information is rarely available due to limited and noisy measurements
- **Goal** $\Rightarrow$ develop reliable methods for **estimating traffic from partial data**

Traffic Flow Modeling Scales

Benchmark scales of traffic models

- microscopic $\Rightarrow$ individual vehicle dynamics, full information given

Microscopic model

- Simulation of agent-based dynamics
- Tracking position $x_i(t)$, velocity $v_i(t)$ of vehicle i at time t
- Each driver responds to surrounding traffic by adjusting his speed

$$\dot{v}_i(t) = F(v_i(t), x_i(t)) \qquad (1)$$

Traffic Flow Modeling Scales

Benchmark scales of traffic models

- macroscopic $\Rightarrow$ continuum representation using aggregated variables

Macroscopic model

- Traffic modelled as a continuous flow
- Density $\rho(t,x)$, speed $v(\rho)$, flux $f(\rho)$
- Total number of cars is conserved

$$\begin{aligned} 0 =& \frac{d}{dt}\int_a^b \rho(t,x)dx \\ =& f(\rho(t,a)) - f(\rho(t,b)) \\ =& -\int_a^b \frac{\partial}{\partial x} f(\rho(t,x))dx \end{aligned} \tag{2}$$

Traffic Flow Modeling Scales

Benchmark scales of traffic models

- microscopic $\Rightarrow$ individual vehicle dynamics, full information given
- macroscopic $\Rightarrow$ continuum representation using aggregated variables

Microscopic model

- Simulation of agent-based dynamics
- Tracking position $x_i(t)$, velocity $v_i(t)$ of vehicle i at time t
- Each driver responds to surrounding traffic by adjusting his speed

$$\dot{v}_i(t) = F(v_i(t), x_i(t)) \qquad (1)$$

Macroscopic model

- Traffic modelled as a continuous flow
- Density $\rho(t,x)$, speed $v(\rho)$, flux $f(\rho)$
- Total number of cars is conserved

$$\begin{aligned} 0 =& \frac{d}{dt}\int_a^b \rho(t,x)dx \\ =& f(\rho(t,a)) - f(\rho(t,b)) \qquad (2) \\ =& -\int_a^b \frac{\partial}{\partial x} f(\rho(t,x))dx \end{aligned}$$

- **Connection** $\Rightarrow$ macroscopic variables emerge from microscopic interactions

Table of Contents

Model-Based Approaches

- Follow-the-Leader (FtL), **microscopic** first order model
  $\Rightarrow$ dynamics of each vehicle depend on vehicle immediately in front

$$\begin{cases} \dot{x}_N^N(t) = v_{\max}, & t > 0, \\ \dot{x}_i^N(t) = v\left(\frac{L}{N(x_{i+1}^N(t) - x_i^N(t))}\right), & t > 0, \quad i = 0, \cdots, N-1 \\ x_i^N(0) = \bar{x}_i^N, & i = 0, \cdots, N \end{cases} \tag{3}$$

  $\Rightarrow$ accurate traffic representation, encodes individual movements
  $\Rightarrow$ computationally demanding, requires more data

Model-Based Approaches

- Follow-the-Leader (FtL), **microscopic** first order model
  $\Rightarrow$ dynamics of each vehicle depend on vehicle immediately in front

$$\begin{cases} \dot{x}_N^N(t) = v_{\max}, & t > 0, \\ \dot{x}_i^N(t) = v\left(\frac{L}{N(x_{i+1}^N(t) - x_i^N(t))}\right), & t > 0, \quad i = 0, \cdots, N-1 \\ x_i^N(0) = \bar{x}_i^N, & i = 0, \cdots, N \end{cases} \tag{3}$$

  $\Rightarrow$ accurate traffic representation, encodes individual movements
  $\Rightarrow$ computationally demanding, requires more data

- Lighthill-William-Richards (LWR), **macroscopic** traffic flow model
  $\Rightarrow$ vehicles treated as a continuous medium similar to particles in fluid
  $\Rightarrow$ one-dimensional (hyperbolic) conservation law

$$\begin{cases} \frac{\partial}{\partial t}\rho(t,x) + \frac{\partial}{\partial x} f(\rho(t,x)) = 0, & x \in \mathbb{R}, \quad t > 0, \\ \rho(x,0) = \rho_0(x), & x \in \mathbb{R} \end{cases} \tag{4}$$

  $\Rightarrow$ faster implementation, less data-intensive
  $\Rightarrow$ overlooks traffic heterogeneity, oversimplifies traffic phenomena

Model-Based Approaches

- **Convergence analysis of FtL approximation scheme towards LWR model**[1]

[1] **holden˙continuum˙2017**.
[2] **francesco˙rigorous˙2015**.

- **Convergence analysis of FtL approximation scheme towards LWR model**[1]
- Link between FtL and LWR based on atomization of initial density ρ_0

$$\bar{x}_{i+1}^N := \sup\left\{ x \in \mathbb{R} : \int_{\bar{x}_i^N}^{x} \rho_0(y)dy = \frac{L}{N} \right\}, \quad i = 0, \cdots, N-1 \tag{5}$$

[1] **holden˙continuum˙2017**.
[2] **francesco˙rigorous˙2015**.

- **Convergence analysis of FtL approximation scheme towards LWR model**[1]
- Link between FtL and LWR based on atomization of initial density ρ_0

$$\bar{x}_{i+1}^N := \sup\left\{ x \in \mathbb{R} : \int_{\bar{x}_i^N}^{x} \rho_0(y)dy = \frac{L}{N} \right\}, \quad i = 0, \cdots, N-1 \tag{5}$$

- Solution of PDE (3) can be recovered as many particle limit[2] of ODE system (4)

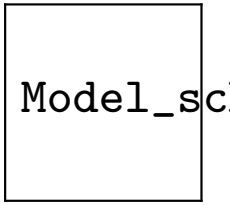

Coupled Resolution of a Microscopic ODE System and a Macroscopic PDE

[1] **holden˙continuum˙2017**.
[2] **francesco˙rigorous˙2015**.

- Hybrid micro-macro models explored in traffic density reconstruction[3]

$$\begin{cases} \dot{x}_N^N(t) = v_{\max}, & t > 0, \\ \dot{x}_i^N(t) = v\left(\rho(t, x_i^N(t))\right), & t > 0, , \quad i = 0, \cdots, N-1 \\ \frac{\partial}{\partial t}\rho(t,x) + \frac{\partial}{\partial x} f(\rho(t,x)) = \gamma^2 \frac{\partial^2}{\partial x^2}\rho(t,x), & x \in \mathbb{R}, \quad t > 0, \end{cases} \tag{6}$$

[3] **barreau˙physics-informed˙2021**.
[4] **liu˙learning-based˙2020**.

- Hybrid micro-macro models explored in traffic density reconstruction[3]

$$\begin{cases} \dot{x}_N^N(t) = v_{\max}, & t > 0, \\ \dot{x}_i^N(t) = v\left(\rho(t, x_i^N(t))\right), & t > 0, , \quad i = 0, \cdots, N-1 \\ \frac{\partial}{\partial t}\rho(t,x) + \frac{\partial}{\partial x} f(\rho(t,x)) = \gamma^2 \frac{\partial^2}{\partial x^2}\rho(t,x), & x \in \mathbb{R}, \quad t > 0, \end{cases} \tag{6}$$

- **Partial state reconstruction**[4] using measurements from probe vehicles (PVs)
  $\Rightarrow$ low penetration rate $N_{\text{probes}} \ll N_{\text{total}}$
  $\Rightarrow$ recover density ρ from **limited** trajectories

[3] **barreau˙physics-informed˙2021**.
[4] **liu˙learning-based˙2020**.

- Hybrid micro-macro models explored in traffic density reconstruction[3]

$$\begin{cases} \dot{x}_N^N(t) = v_{\max}, & t > 0, \\ \dot{x}_i^N(t) = v\left(\rho(t, x_i^N(t))\right), & t > 0, , \quad i = 0, \cdots, N-1 \\ \frac{\partial}{\partial t}\rho(t,x) + \frac{\partial}{\partial x} f(\rho(t,x)) = \gamma^2 \frac{\partial^2}{\partial x^2}\rho(t,x), & x \in \mathbb{R}, \quad t > 0, \end{cases} \tag{6}$$

- **Partial state reconstruction**[4] using measurements from probe vehicles (PVs)
  $\Rightarrow$ low penetration rate $N_{\text{probes}} \ll N_{\text{total}}$
  $\Rightarrow$ recover density ρ from **limited** trajectories
- Requires access to real-time positions, densities and instantaneous speeds of PVs

[3] **barreau˙physics-informed˙2021**.
[4] **liu˙learning-based˙2020**.

- Hybrid micro-macro models explored in traffic density reconstruction[3]

$$\begin{cases} \dot{x}_N^N(t) = v_{\max}, & t > 0, \\ \dot{x}_i^N(t) = v\left(\rho(t, x_i^N(t))\right), & t > 0, , \quad i = 0, \cdots, N-1 \\ \frac{\partial}{\partial t}\rho(t,x) + \frac{\partial}{\partial x} f(\rho(t,x)) = \gamma^2 \frac{\partial^2}{\partial x^2}\rho(t,x), & x \in \mathbb{R}, \quad t > 0, \end{cases} \tag{6}$$

- **Partial state reconstruction**[4] using measurements from probe vehicles (PVs)
  $\Rightarrow$ low penetration rate $N_{\text{probes}} \ll N_{\text{total}}$
  $\Rightarrow$ recover density ρ from **limited** trajectories
- Requires access to real-time positions, densities and instantaneous speeds of PVs
- Prior approaches rely on knowledge of initial density ρ_0
  $\Rightarrow$ **No access** to this critical information, need to leverage available data

[3] **barreau˙physics-informed˙2021**.
[4] **liu˙learning-based˙2020**.

Table of Contents

Parametrized Microscopic Model

- **Limited data scenario** $\Rightarrow$ only **initial and final** $\left\{\left(\bar{x}^N, \bar{y}^N\right)\right\}_{i=0}^{n}$ positions of PVs

Parametrized Microscopic Model

- **Limited data scenario** $\Rightarrow$ only **initial and final** $\left\{\left(\bar{x}^N, \bar{y}^N\right)\right\}_{i=0}^{n}$ positions of PVs
- **Enhanced** version of FtL scheme (3) adding a parameter
  $\Rightarrow$ α^N accounts for unobserved vehicles between consecutive PVs
  $\Rightarrow$ adjusts dynamics and allows varying levels of response
  $\Rightarrow$ bridges discrete (vehicle-level) dynamics to continuous (density-level) dynamics

Parametrized Microscopic Model

- **Limited data scenario** $\Rightarrow$ only **initial and final** $\left\{\left(\bar{x}^N, \bar{y}^N\right)\right\}_{i=0}^{n}$ positions of PVs
- **Enhanced** version of FtL scheme (3) adding a parameter
  $\Rightarrow$ α^N accounts for unobserved vehicles between consecutive PVs
  $\Rightarrow$ adjusts dynamics and allows varying levels of response
  $\Rightarrow$ bridges discrete (vehicle-level) dynamics to continuous (density-level) dynamics
- Parametrized ODE system with finite time horizon

$$\begin{cases} \dot{x}_n^N(t) = v_{\max}, & t \in (0, T] \\ \dot{x}_i^N(t) = v\left(\rho_i^N(t)\right), & t \in (0, T] \quad i = 0, \cdots, n-1 \\ x_i^N(0) = \bar{x}_i^N, & i = 0, \cdots, n \end{cases} \tag{7}$$

  $\Rightarrow$ local discrete densities

$$\rho_i^N(t) := \frac{\alpha_i^N L}{N\left(x_{i+1}^N(t) - x_i^N(t)\right)}, \quad t \in (0, T], \quad i = 0, \cdots, n-1 \tag{8}$$

Parametrized Microscopic Model

- **Limited data scenario** $\Rightarrow$ only **initial and final** $\left\{\left(\bar{x}^N, \bar{y}^N\right)\right\}_{i=0}^{n}$ positions of PVs
- **Enhanced** version of FtL scheme (3) adding a parameter
  $\Rightarrow$ α^N accounts for unobserved vehicles between consecutive PVs
  $\Rightarrow$ adjusts dynamics and allows varying levels of response
  $\Rightarrow$ bridges discrete (vehicle-level) dynamics to continuous (density-level) dynamics
- Parametrized ODE system with finite time horizon

$$\begin{cases} \dot{x}_n^N(t) = v_{\max}, & t \in (0, T] \\ \dot{x}_i^N(t) = v\left(\rho_i^N(t)\right), & t \in (0, T] \quad i = 0, \cdots, n-1 \\ x_i^N(0) = \bar{x}_i^N, & i = 0, \cdots, n \end{cases} \tag{7}$$

  $\Rightarrow$ local discrete densities

$$\rho_i^N(t) := \frac{\alpha_i^N L}{N\left(x_{i+1}^N(t) - x_i^N(t)\right)}, \quad t \in (0, T], \quad i = 0, \cdots, n-1 \tag{8}$$

- Piecewise constant Eulerian discrete density

$$\rho^N(t, x) := \sum_{i=0}^{N-1} \rho_i^N(t) \chi_{[x_i^N(t), x_{i+1}^N(t))}(x), \quad x \in \mathbb{R}, \quad t \in [0, T] \tag{9}$$

Well Posedness

- Assumptions on velocity

$$v \in C^1([0, +\infty)) \tag{10a}$$
$$v \text{ is decreasing on } [0, +\infty) \tag{10b}$$
$$v(0) = v_{\max} < \infty \tag{10c}$$

[5] **francesco˙follow-leader˙2016**.

Well Posedness

- Assumptions on velocity

$$v \in C^1([0, +\infty)) \tag{10a}$$
$$v \text{ is decreasing on } [0, +\infty) \tag{10b}$$
$$v(0) = v_{\max} < \infty \tag{10c}$$

- Local existence and uniqueness of solution to (7) (for fixed α) via Picard-Lindelöf

[5] **francesco˙follow-leader˙2016**.

Well Posedness

- Assumptions on velocity

$$v \in C^1([0, +\infty)) \tag{10a}$$
$$v \text{ is decreasing on } [0, +\infty) \tag{10b}$$
$$v(0) = v_{\max} < \infty \tag{10c}$$

- Local existence and uniqueness of solution to (7) (for fixed α) via Picard-Lindelöf
- Condition on initial car positions $\bar{x}_0^N < \bar{x}_1^N < \cdots < \bar{x}_{n-1}^N < \bar{x}_n^N$
  $\Rightarrow$ global existence

Lemma (Discrete maximum principle)

For solution $x(t)$ of (7) with v satisfying (10a)-(10c), for all $i = 0, \cdots, n-1$,

$$\frac{\alpha_i^N L}{NM} \leq x_{i+1}^N(t) - x_i^N(t) \leq \bar{x}_n^N - \bar{x}_0^N + (v_{\max} - v(M))\, t, \quad \forall t \in [0, T], \tag{11}$$

where $M := \max_i \left(\frac{\alpha_i^N L}{N(\bar{x}_{i+1}^N - \bar{x}_i^N)} \right)$

[5] **francesco˙follow-leader˙2016**.

Well Posedness

- Assumptions on velocity

$$v \in C^1([0, +\infty)) \tag{10a}$$
$$v \text{ is decreasing on } [0, +\infty) \tag{10b}$$
$$v(0) = v_{\max} < \infty \tag{10c}$$

- Local existence and uniqueness of solution to (7) (for fixed α) via Picard-Lindelöf
- Condition on initial car positions $\bar{x}_0^N < \bar{x}_1^N < \cdots < \bar{x}_{n-1}^N < \bar{x}_n^N$
  $\Rightarrow$ global existence

Lemma (Discrete maximum principle)

For solution $x(t)$ of (7) with v satisfying (10a)-(10c), for all $i = 0, \cdots, n-1$,

$$\frac{\alpha_i^N L}{NM} \leq x_{i+1}^N(t) - x_i^N(t) \leq \bar{x}_n^N - \bar{x}_0^N + (v_{\max} - v(M))\, t, \quad \forall t \in [0, T], \tag{11}$$

where $M := \max_i \left(\frac{\alpha_i^N L}{N(\bar{x}_{i+1}^N - \bar{x}_i^N)} \right)$

- ρ^N discrete approximation[5] of solution to LWR model (4)

[5] **francesco˙follow-leader˙2016**.

ODE-Contrained Optimization

- Physical conditions on $\alpha := \alpha^N$ induce feasible set

$$\mathcal{A}_N := \left\{ \alpha \in \mathbb{R}^n : \quad \alpha_i \in \left[1, \bar{z}_i^N\right], \quad i = 0, \dots, n-1, \quad \sum_{i=0}^{n-1} \alpha_i = N \right\} \tag{12}$$

with $\bar{z}_i^N := \min \left\{ \frac{N\left(\bar{x}_{i+1}^N - \bar{x}_i^N\right)}{L}, \frac{N\left(\bar{y}_{i+1}^N - \bar{y}_i^N\right)}{L} \right\}, \quad i = 0, \dots, n-1$

[6] **baloul˙reconstruction˙2025**.

ODE-Contrained Optimization

- Physical conditions on $\alpha := \alpha^N$ induce feasible set

$$\mathcal{A}_N := \left\{ \alpha \in \mathbb{R}^n : \quad \alpha_i \in \left[1, \bar{z}_i^N\right], \quad i = 0, \dots, n-1, \quad \sum_{i=0}^{n-1} \alpha_i = N \right\} \tag{12}$$

with $\bar{z}_i^N := \min \left\{ \frac{N\left(\bar{x}_{i+1}^N - \bar{x}_i^N\right)}{L}, \frac{N\left(\bar{y}_{i+1}^N - \bar{y}_i^N\right)}{L} \right\}, \quad i = 0, \dots, n-1$

- **Approximate density reconstruction**[6] $\Rightarrow$ find optimal interaction parameter α

$$\begin{aligned} & \underset{\alpha}{\text{minimize}} \quad \frac{1}{2} \left\| x(T) - \bar{y} \right\|^2 \\ \text{s.t.} \quad & \dot{x}(t) = V\left(W_\alpha x(t) + b_\alpha(t)\right) \\ & x(0) = \bar{x} \\ & \alpha \in \mathcal{A}_N \end{aligned} \tag{13}$$

[6] **baloul˙reconstruction˙2025**.

ODE-Contrained Optimization

- Physical conditions on $\alpha := \alpha^N$ induce feasible set

$$\mathcal{A}_N := \left\{ \alpha \in \mathbb{R}^n : \quad \alpha_i \in \left[1, \bar{z}_i^N\right], \quad i = 0, \dots, n-1, \quad \sum_{i=0}^{n-1} \alpha_i = N \right\} \tag{12}$$

with $\bar{z}_i^N := \min \left\{ \frac{N\left(\bar{x}_{i+1}^N - \bar{x}_i^N\right)}{L}, \frac{N\left(\bar{y}_{i+1}^N - \bar{y}_i^N\right)}{L} \right\}, \quad i = 0, \dots, n-1$

- **Approximate density reconstruction**[6] $\Rightarrow$ find optimal interaction parameter α

$$\begin{aligned} \underset{\alpha}{\text{minimize}} \quad & \frac{1}{2} \left\| x(T) - \bar{y} \right\|^2 \\ \text{s.t.} \quad & \dot{x}(t) = V\left(W_\alpha x(t) + b_\alpha(t)\right) \\ & x(0) = \bar{x} \\ & \alpha \in \mathcal{A}_N \end{aligned} \tag{13}$$

- Existence of solutions guaranteed by assumptions on $V := v \circ \frac{1}{\cdot}$ (continuity of v) and constraints on α (compactness of $\mathcal{A}_N$)

[6] **baloul˙reconstruction˙2025**.

ODE-Contrained Optimization

- Physical conditions on $\alpha := \alpha^N$ induce feasible set

$$\mathcal{A}_N := \left\{ \alpha \in \mathbb{R}^n : \quad \alpha_i \in \left[1, \bar{z}_i^N\right], \quad i = 0, \dots, n-1, \quad \sum_{i=0}^{n-1} \alpha_i = N \right\} \tag{12}$$

with $\bar{z}_i^N := \min \left\{ \frac{N\left(\bar{x}_{i+1}^N - \bar{x}_i^N\right)}{L}, \frac{N\left(\bar{y}_{i+1}^N - \bar{y}_i^N\right)}{L} \right\}, \quad i = 0, \dots, n-1$

- **Approximate density reconstruction**[6] $\Rightarrow$ find optimal interaction parameter α

$$\begin{aligned} \underset{\alpha}{\text{minimize}} \quad & \frac{1}{2} \left\| x(T) - \bar{y} \right\|^2 \\ \text{s.t.} \quad & \dot{x}(t) = V\left(W_\alpha x(t) + b_\alpha(t)\right) \\ & x(0) = \bar{x} \\ & \alpha \in \mathcal{A}_N \end{aligned} \tag{13}$$

- Existence of solutions guaranteed by assumptions on $V := v \circ \frac{1}{\cdot}$ (continuity of v) and constraints on α (compactness of $\mathcal{A}_N$)
- No uniqueness (a priori) since nonlinear dynamics can lead to multiple minima

[6] **baloul˙reconstruction˙2025**.

Learning Method

- Dataset consists of **artificial data** based on simulated (classical) FtL dynamics (3)
- Sampling of PVs yielding a **balanced representation** of overall traffic

Learning Method

- Dataset consists of **artificial data** based on simulated (classical) FtL dynamics (3)
- Sampling of PVs yielding a **balanced representation** of overall traffic
- Neural network architecture designed to **understand dynamics of traffic**

Learning Method

- Dataset consists of **artificial data** based on simulated (classical) FtL dynamics (3)
- Sampling of PVs yielding a **balanced representation** of overall traffic
- Neural network architecture designed to **understand dynamics of traffic**
- Residual network (ResNet) where each block corresponds to a single time step
- Input $\bar{x}$ and state $x(.)$ is propagated by mirroring Euler discretization

$$x(t + \Delta t) = x(t) + V(Wx(t) + b)\Delta t \tag{14}$$

- Weights and biases W, b are functions of α

$$\begin{cases} W_{i,i} & := -\frac{N}{\alpha_i L}, i = 0, \ldots, n-1, \\ W_{i,i+1} & := \frac{N}{\alpha_i L}, i = 1, \ldots, n-2, \\ W_{i,j} & := 0, \text{otherwise}, \end{cases} \tag{15}$$

$$b_i(t) =:= \delta_{i,n} \frac{N}{\alpha_{n-1} L} \left(v_{\max} t + \bar{x}_n^N \right), \quad t \in [0, T] \tag{16}$$

- Nonlinear dynamic map V acts as physics grounded activation function
- Backpropagation to minimize predictions errors $\frac{1}{n} \sum_{j=0}^{n} |x_j^\alpha(T) - \bar{y}_j^N|^2$

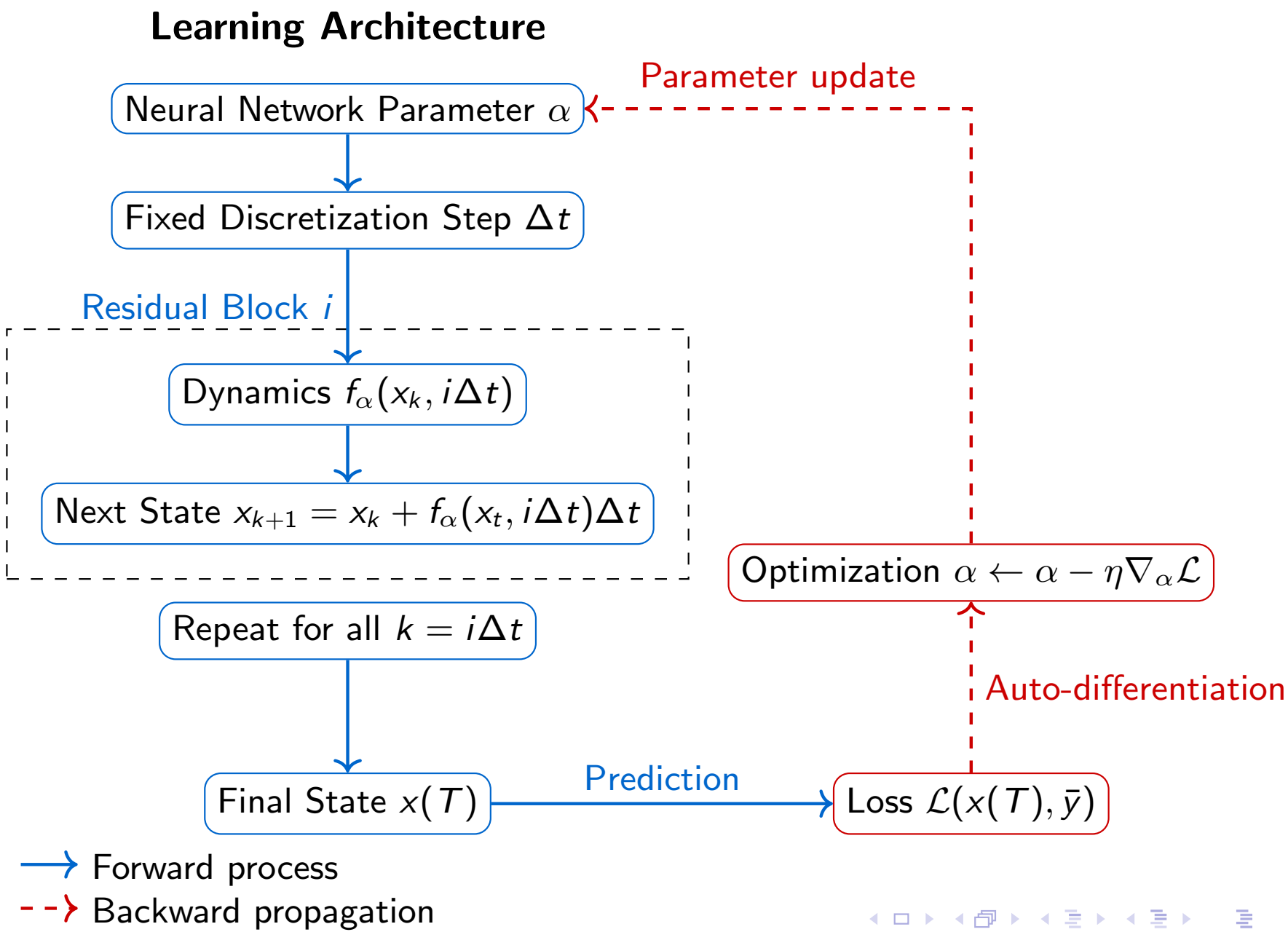
Learning Architecture
Parameter update
Neural Network Parameter α
Fixed Discretization Step Δt
Residual Block i
Dynamics $f_\alpha(x_k, i\Delta t)$
Next State $x_{k+1} = x_k + f_\alpha(x_t, i\Delta t)\Delta t$
Optimization $\alpha \leftarrow \alpha - \eta \nabla_\alpha \mathcal{L}$
Repeat for all $k = i\Delta t$
Auto-differentiation
Final State $x(T)$
Prediction
Loss $\mathcal{L}(x(T), \bar{y})$
Forward process
Backward propagation

Model validation

- Through optimal parameter $\bar{\alpha}$, training yields piecewise constant discrete density

$$\rho^N(t,x) = \sum_{i=0}^{n-1} \frac{\bar{\alpha}_i L}{N(x_{i+1}^N(t) - x_i^N(t))} \chi_{[x_i^N(t), x_{i+1}^N(t))}(x), \quad x \in \mathbb{R}, \quad t \in [0,T], \qquad (17)$$

Model validation

- Through optimal parameter $\bar{\alpha}$, training yields piecewise constant discrete density

$$\rho^N(t,x) = \sum_{i=0}^{n-1} \frac{\bar{\alpha}_i L}{N(x_{i+1}^N(t) - x_i^N(t))} \chi_{[x_i^N(t), x_{i+1}^N(t))}(x), \quad x \in \mathbb{R}, \quad t \in [0,T], \tag{17}$$

- Simulation on **test data** by solving ODE system

$$\begin{cases} \dot{x}_i^N(t) = v\left(\rho^N(t, x_i(t)^+)\right), & t \in (0,T], \\ x_i^N(0) = \bar{x}_i^N & i = 0, \dots, n_{\text{test}} \end{cases} \tag{18}$$

Model validation

- Through optimal parameter $\bar{\alpha}$, training yields piecewise constant discrete density

$$\rho^N(t,x) = \sum_{i=0}^{n-1} \frac{\bar{\alpha}_i L}{N(x_{i+1}^N(t) - x_i^N(t))} \chi_{[x_i^N(t), x_{i+1}^N(t))}(x), \quad x \in \mathbb{R}, \quad t \in [0,T], \tag{17}$$

- Simulation on **test data** by solving ODE system

$$\begin{cases} \dot{x}_i^N(t) = v\left(\rho^N(t, x_i(t)^+)\right), & t \in (0,T], \\ x_i^N(0) = \bar{x}_i^N & i = 0, \dots, n_{\text{test}} \end{cases} \tag{18}$$

- Assess model's performance by measuring test error $\frac{1}{n_{\text{test}}} \sum_{j=0}^{n_{\text{test}}} |x_j(T) - \bar{y}_i^N|^2$

Numerical experiments

- Parameters
  - Maximum traffic speed $v_{\max} = 120$ km/h
  - Maximum traffic density $\rho_{\max} = 200$ cars/km
  - Greenshields velocity $v(\rho) = v_{\max} \max\left\{1 - \frac{\rho}{\rho_{max}}, 0\right\}, \quad \rho \in [0, \rho_{max}]$
  - Final time horizon $T = 0.1$ h
- Sampling such 10% **of total fleet serve as PVs for training and** 2.5% **for testing**

Numerical experiments

- Parameters
  - Maximum traffic speed $v_{\max} = 120$ km/h
  - Maximum traffic density $\rho_{\max} = 200$ cars/km
  - Greenshields velocity $v(\rho) = v_{\max} \max\left\{1 - \frac{\rho}{\rho_{max}}, 0\right\}, \quad \rho \in [0, \rho_{max}]$
  - Final time horizon $T = 0.1$ h
- Sampling such 10% **of total fleet serve as PVs for training and** 2.5% **for testing**
- Three traffic scenarii modelled
  1. Shock wave represents an abrupt transition in traffic conditions
  2. Rarefaction wave represents a smooth transition in traffic condition
  3. Stop-and-go wave characterized by alternating regions of congestion and free flow

Shock wave scenario

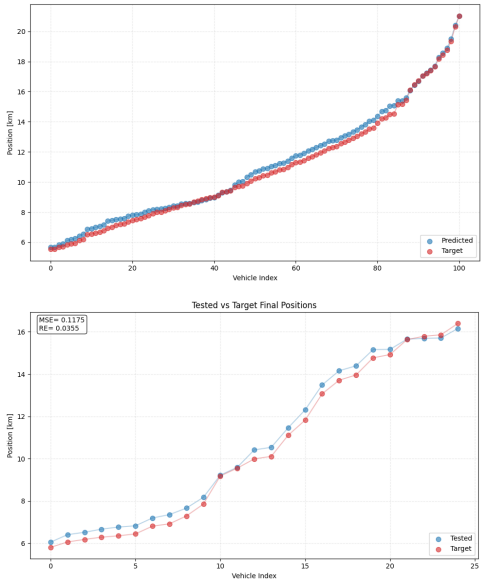

(a) $N = 1000$

Comparison of predicted and target final PV positions
Top Results from **training** procedure
Bottom Results on **test** sounds

Shock wave scenario

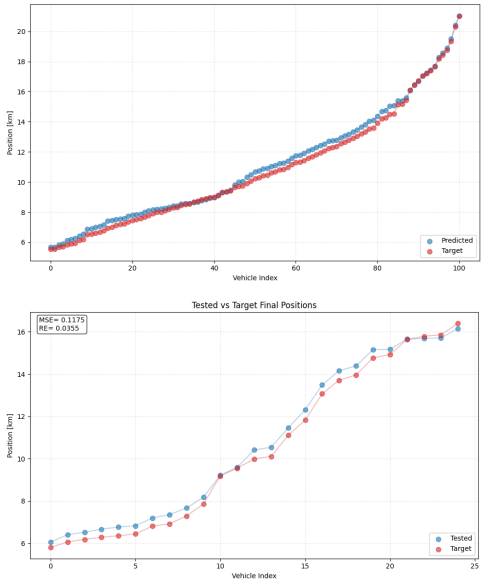

(a) $N = 1000$

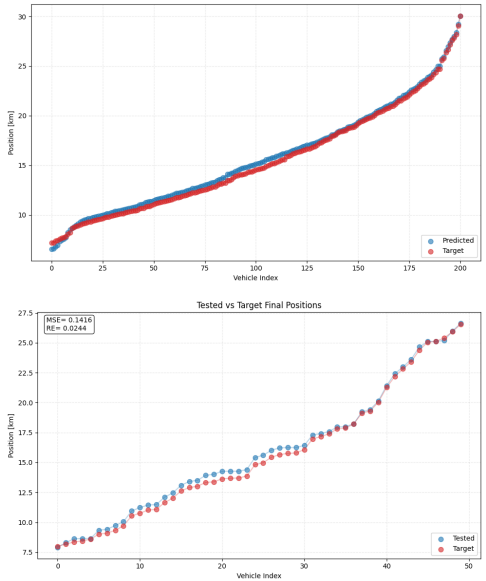

(b) $N = 2000$

Comparison of predicted and target final PV positions
Top Results from **training** procedure
Bottom Results on **test** sounds

Shock wave scenario

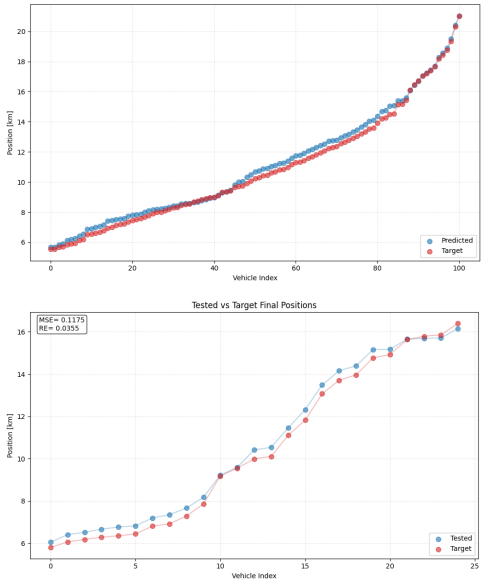

(a) $N = 1000$

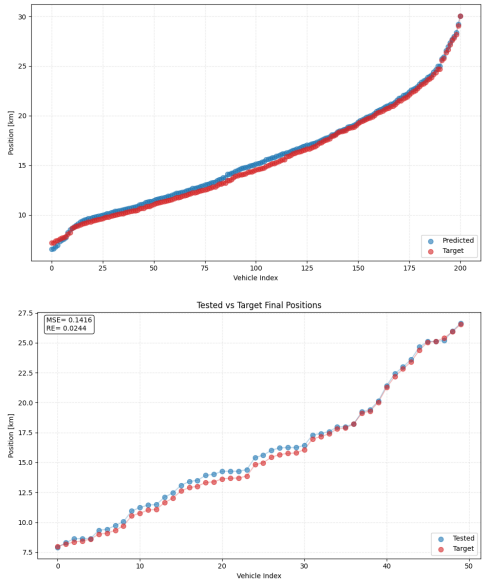

(b) $N = 2000$

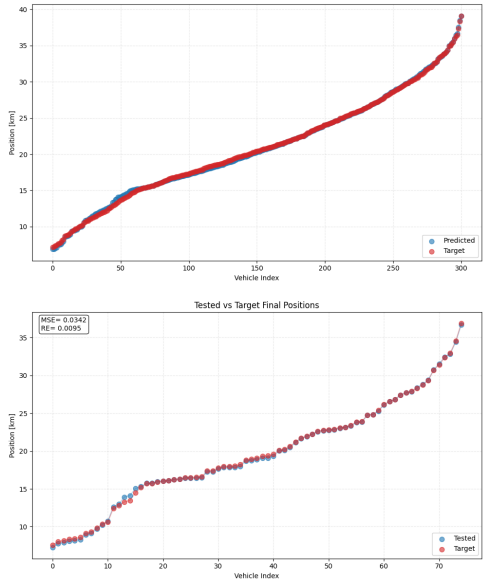

(c) $N = 3000$

Comparison of predicted and target final PV positions
Top Results from **training** procedure
Bottom Results on **test** sounds

Shock wave scenario

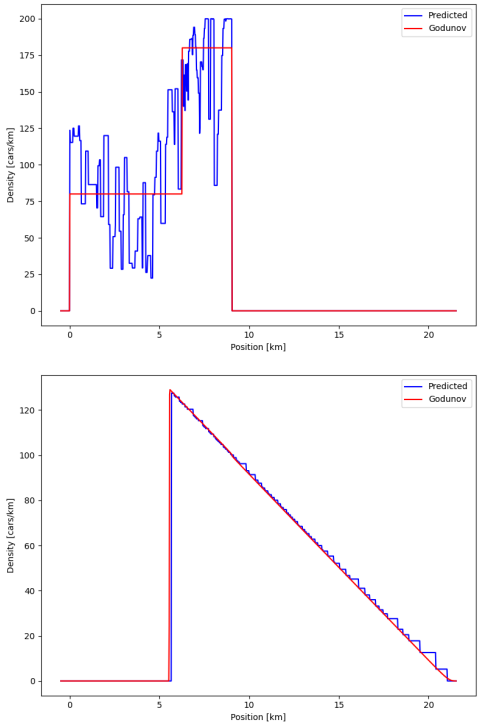

(a) $N = 1000$

Comparison of reconstructed and macroscopic densities
Top Initial densities
Bottom Final densities

Shock wave scenario

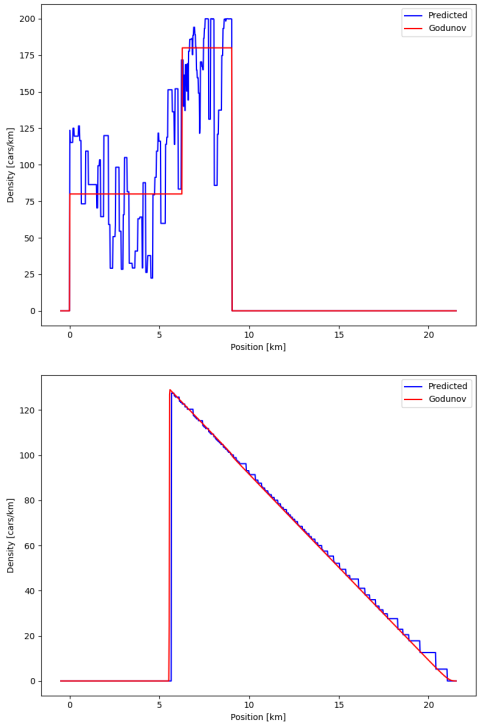

(a) $N = 1000$

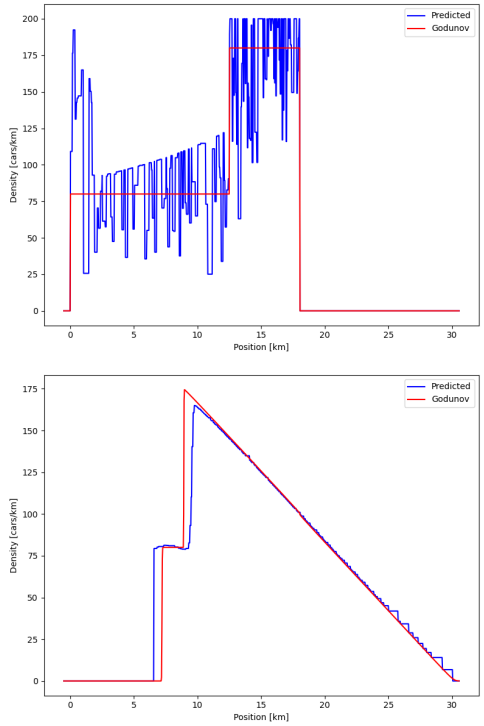

(b) $N = 2000$

Comparison of reconstructed and macroscopic densities
Top Initial densities
Bottom Final densities

Shock wave scenario

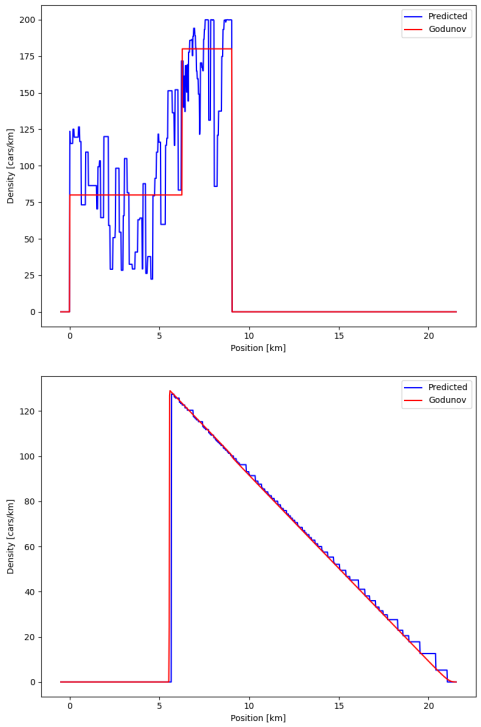

(a) $N = 1000$

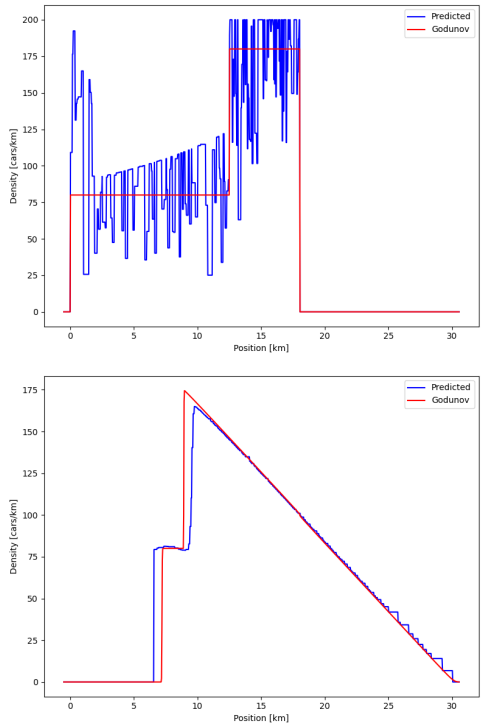

(b) $N = 2000$

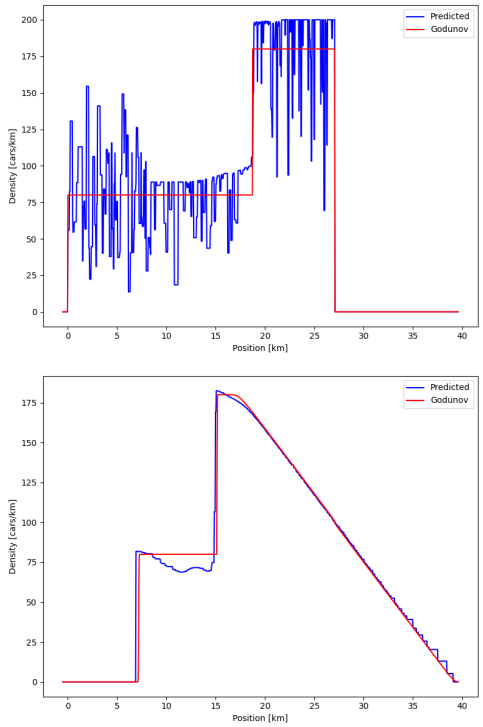

(c) $N = 3000$

Comparison of reconstructed and macroscopic densities
Top Initial densities
Bottom Final densities

Shock wave scenario

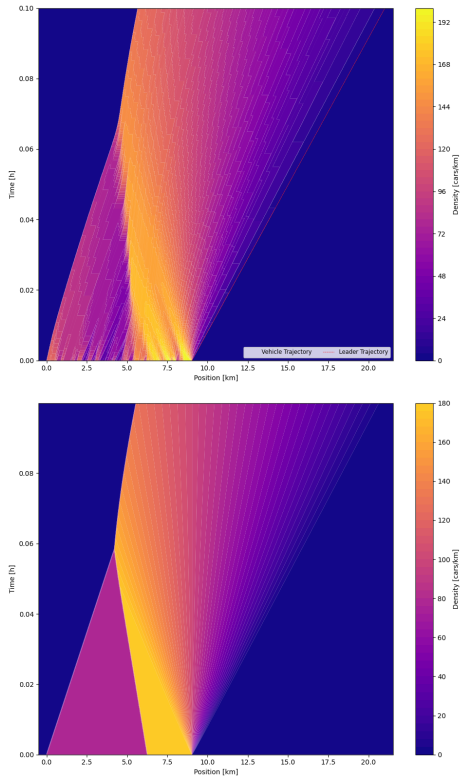

(a) $N = 1000$

Comparison of **reconstructed** and **macroscopic** densities
Top Reconstructed density from learning-based optimization
Bottom Macroscopic density from LWR PDE (Godunov scheme)

Shock wave scenario

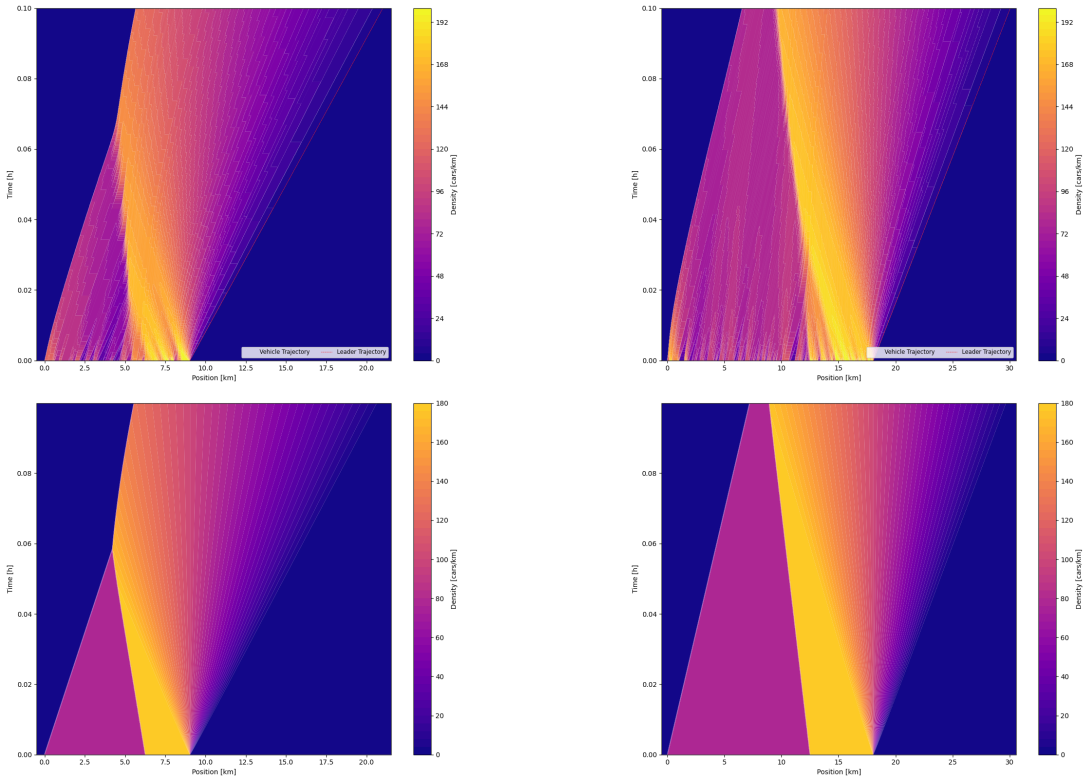

(a) $N = 1000$ (b) $N = 2000$

Comparison of **reconstructed** and **macroscopic** densities
Top Reconstructed density from learning-based optimization
Bottom Macroscopic density from LWR PDE (Godunov scheme)

Shock wave scenario

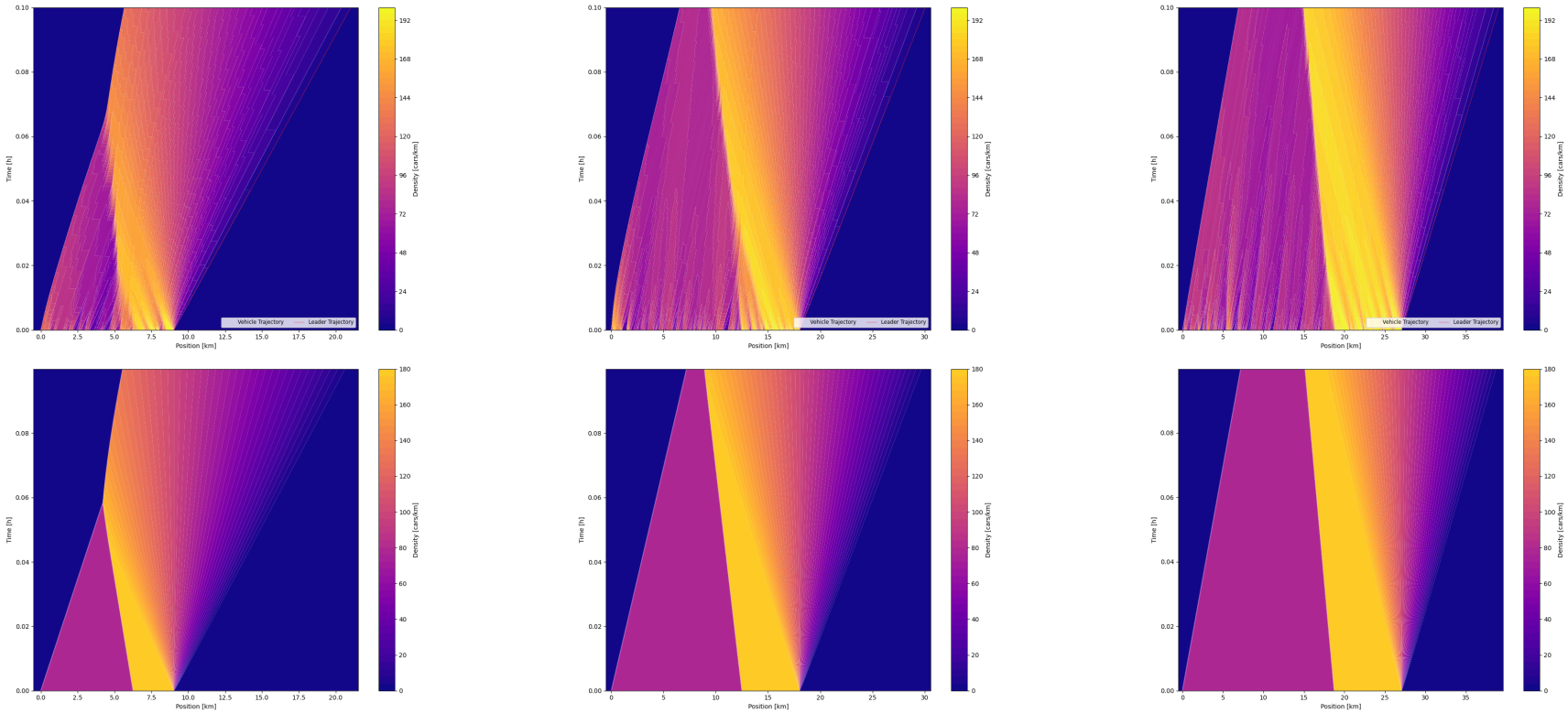

(a) $N = 1000$ (b) $N = 2000$ (c) $N = 3000$

Comparison of **reconstructed** and **macroscopic** densities
Top Reconstructed density from learning-based optimization
Bottom Macroscopic density from LWR PDE (Godunov scheme)

Rarefaction wave scenario

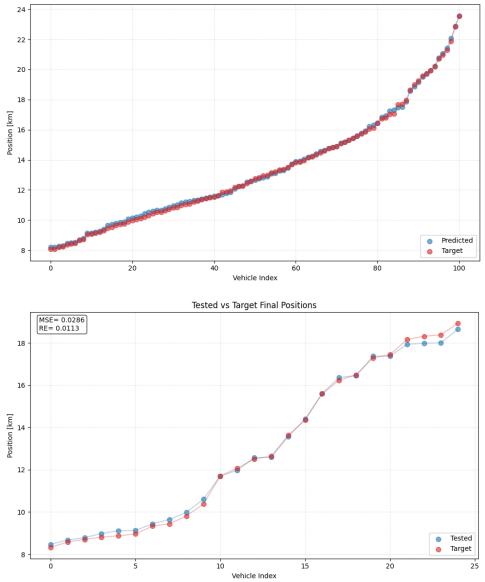

(a) $N = 1000$

Comparison of predicted and target final PV positions
Top Results from **training** procedure
Bottom Results on **test** sounds

Rarefaction wave scenario

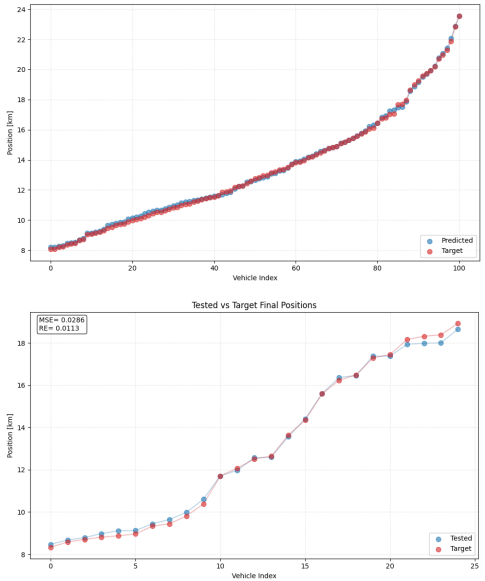

(a) $N = 1000$

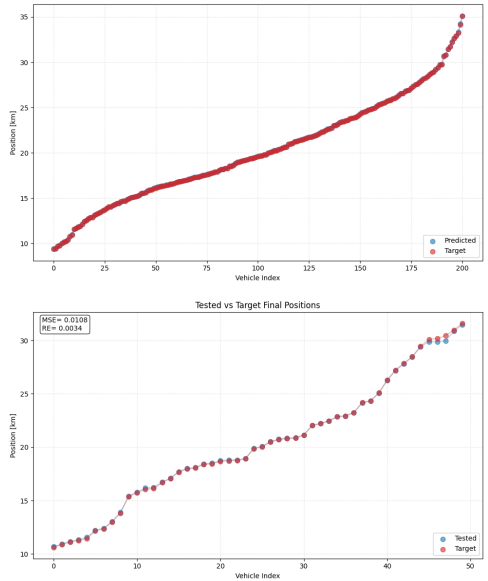

(b) $N = 2000$

Comparison of predicted and target final PV positions
Top Results from **training** procedure
Bottom Results on **test** sounds

Rarefaction wave scenario

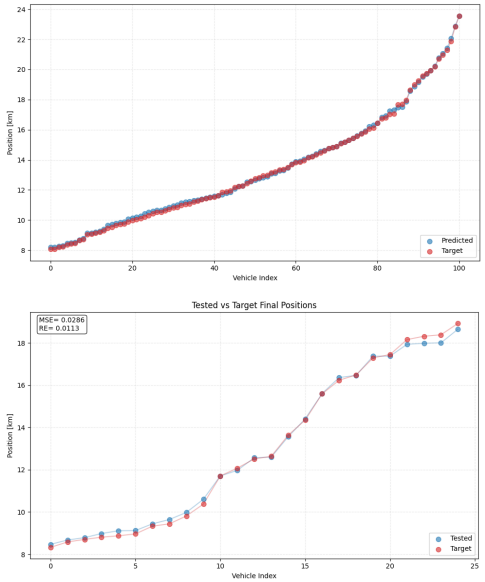

(a) $N = 1000$

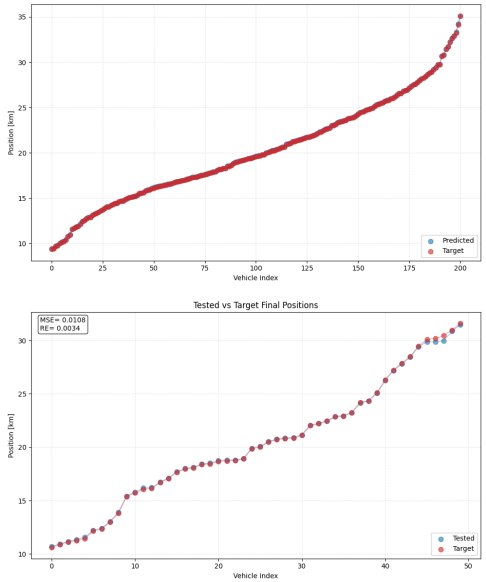

(b) $N = 2000$

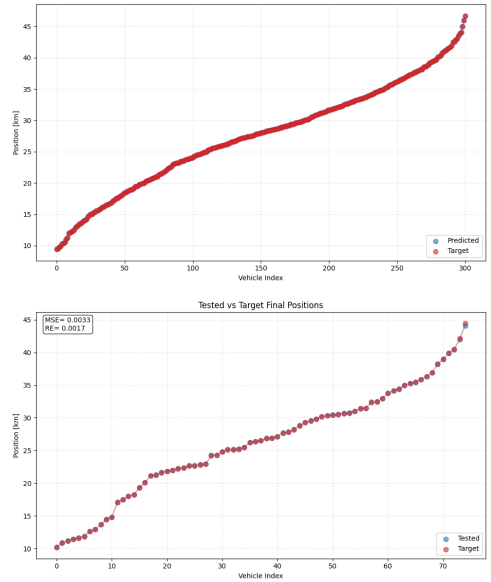

(c) $N = 3000$

Comparison of predicted and target final PV positions
Top Results from **training** procedure
Bottom Results on **test** sounds

Rarefaction wave scenario

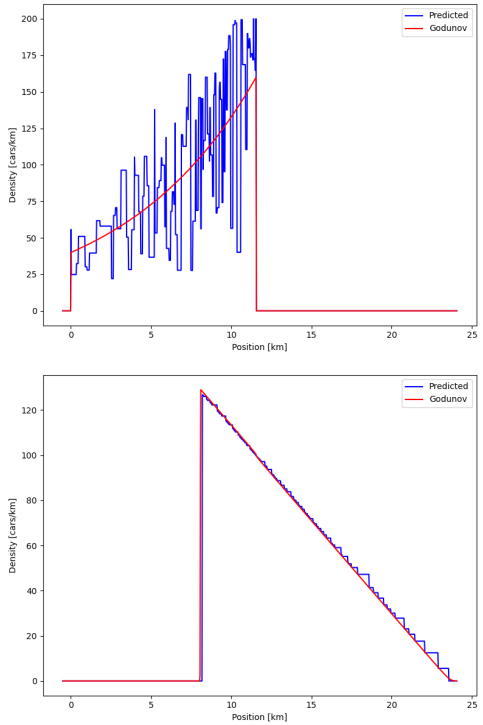

(a) $N = 1000$

Comparison of reconstructed and macroscopic densities
Top Initial densities
Bottom Final densities

Rarefaction wave scenario

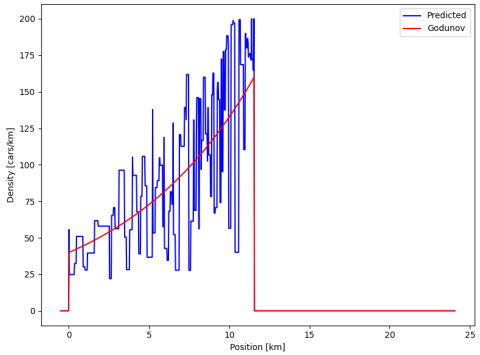

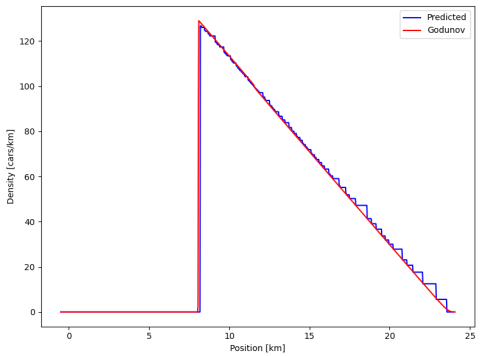

(a) $N = 1000$

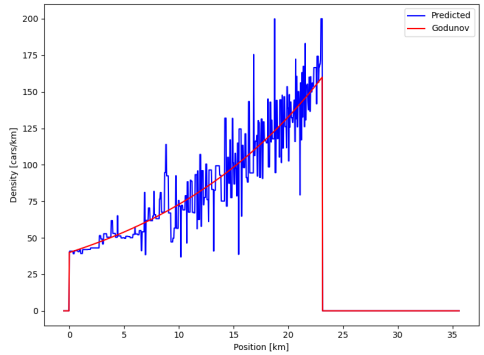

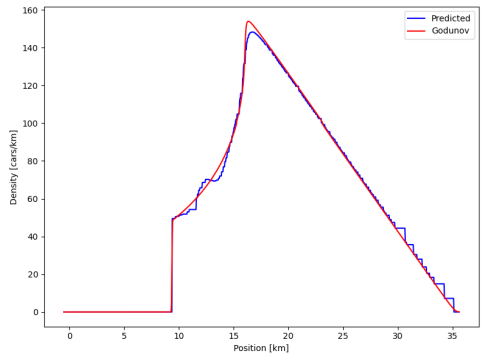

(b) $N = 2000$

Comparison of reconstructed and macroscopic densities
Top Initial densities
Bottom Final densities

Rarefaction wave scenario

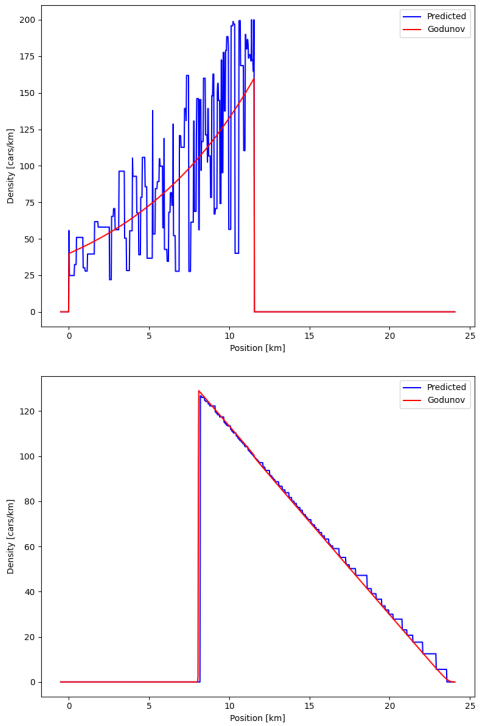

(a) $N = 1000$

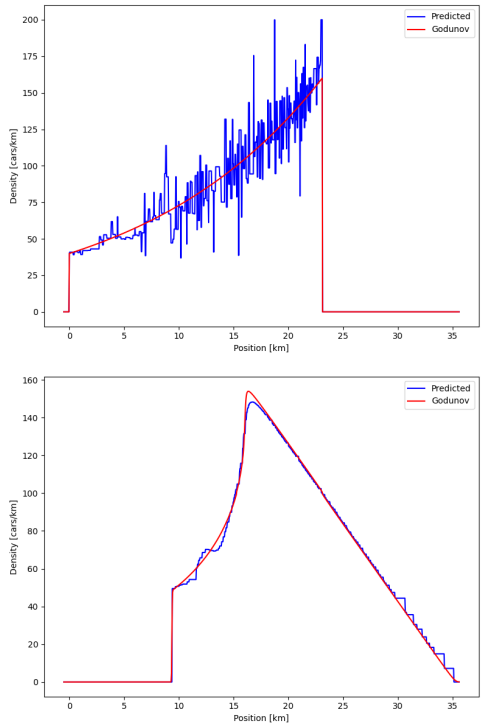

(b) $N = 2000$

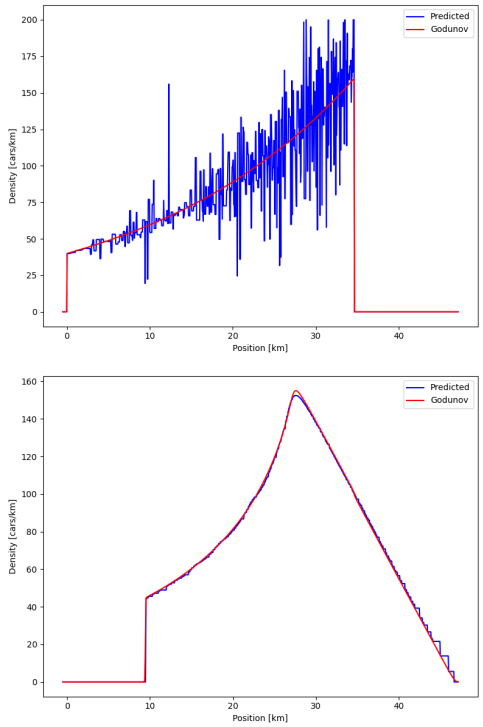

(c) $N = 3000$

Comparison of reconstructed and macroscopic densities
Top Initial densities
Bottom Final densities

Rarefaction wave scenario

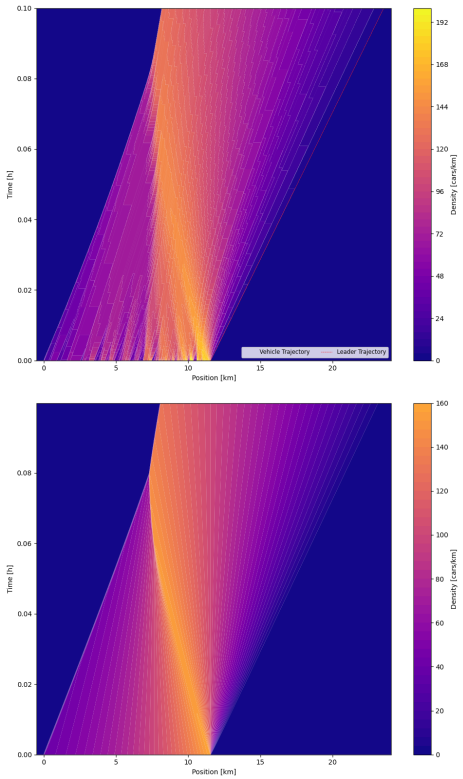

(a) $N = 1000$

Comparison of **reconstructed** and **macroscopic** densities
Top Reconstructed density from learning-based optimization
Bottom Macroscopic density from LWR PDE (Godunov scheme)

Rarefaction wave scenario

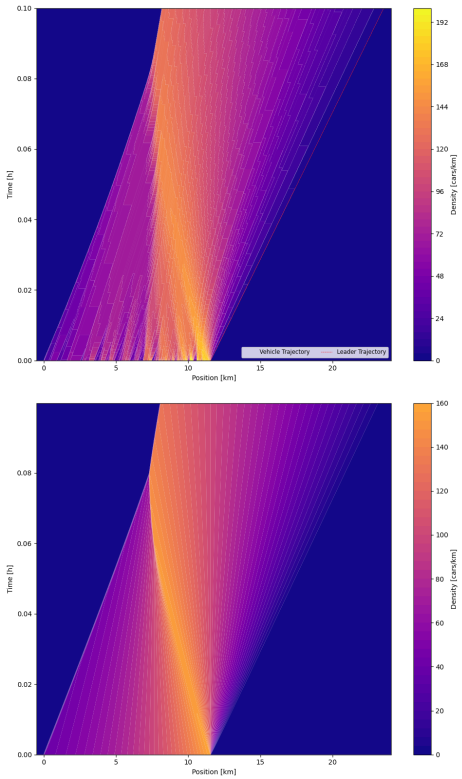

(a) $N = 1000$

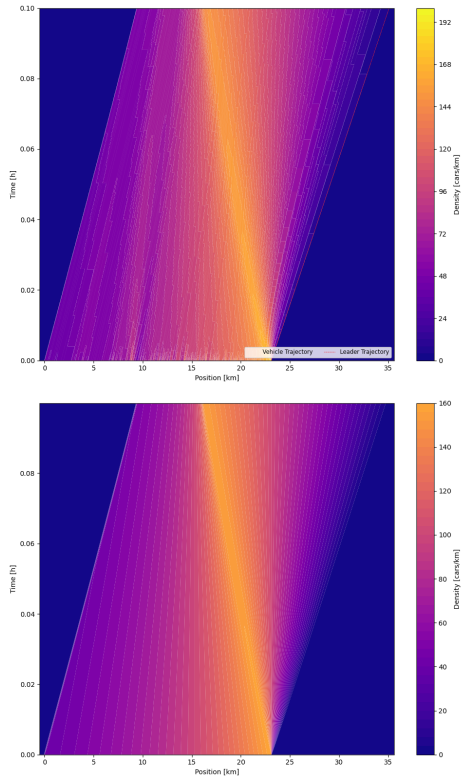

(b) $N = 2000$

Comparison of **reconstructed** and **macroscopic** densities
Top Reconstructed density from learning-based optimization
Bottom Macroscopic density from LWR PDE (Godunov scheme)

Rarefaction wave scenario

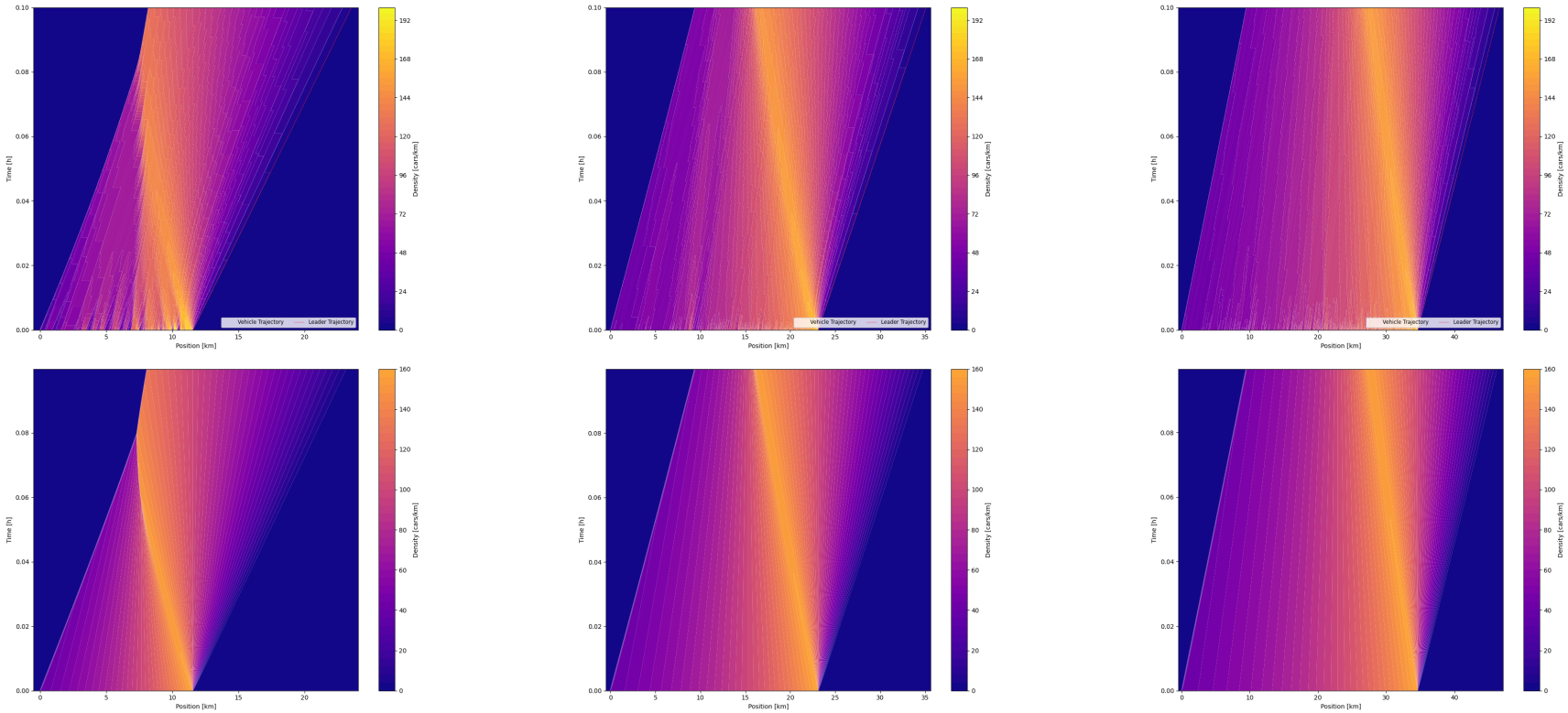

(a) $N = 1000$ (b) $N = 2000$ (c) $N = 3000$

Comparison of **reconstructed** and **macroscopic** densities
Top Reconstructed density from learning-based optimization
Bottom Macroscopic density from LWR PDE (Godunov scheme)

Stop-and-go wave scenario

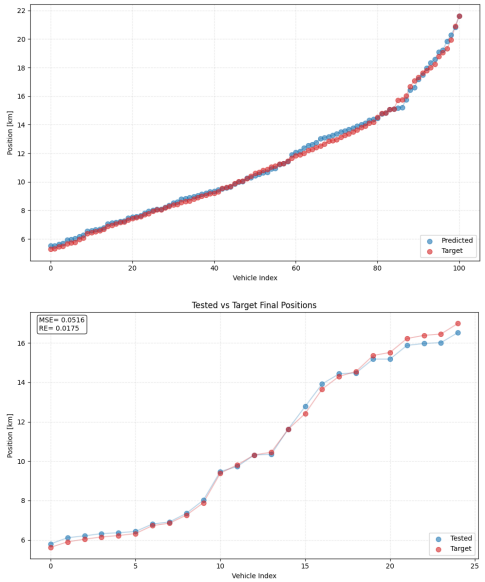

(a) $N = 1000$

Comparison of predicted and target final PV positions
Top Results from **training** procedure
Bottom Results on **test** sounds

Stop-and-go wave scenario

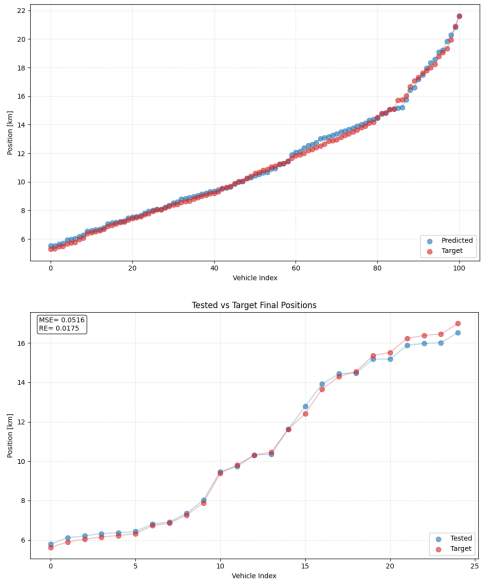

(a) $N = 1000$

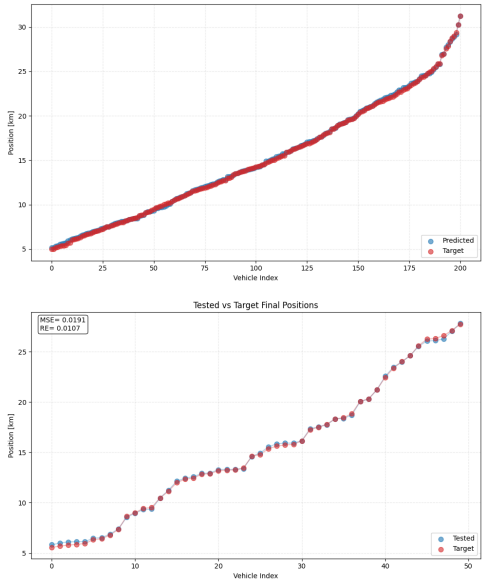

(b) $N = 2000$

Comparison of predicted and target final PV positions
Top Results from **training** procedure
Bottom Results on **test** sounds

Stop-and-go wave scenario

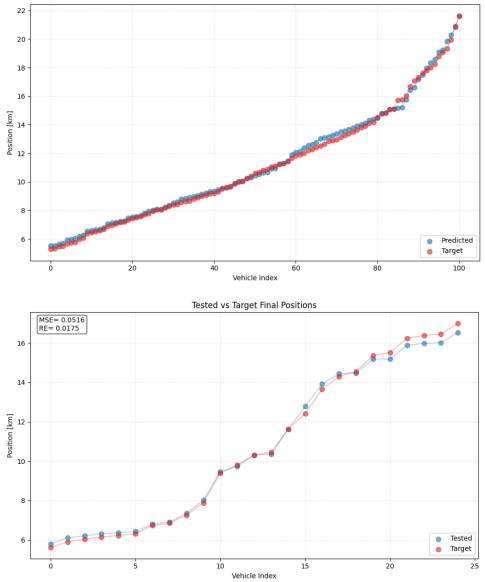

(a) $N = 1000$

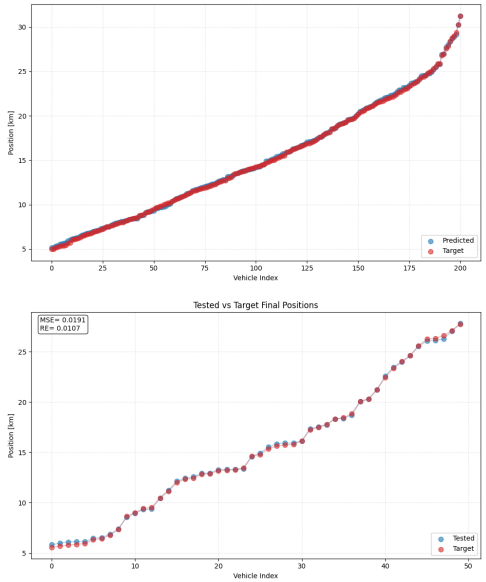

(b) $N = 2000$

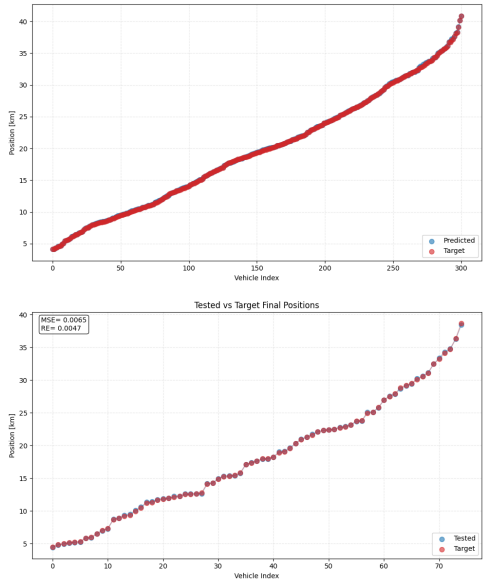

(c) $N = 3000$

Comparison of predicted and target final PV positions
Top Results from **training** procedure
Bottom Results on **test** sounds

Stop-and-go wave scenario

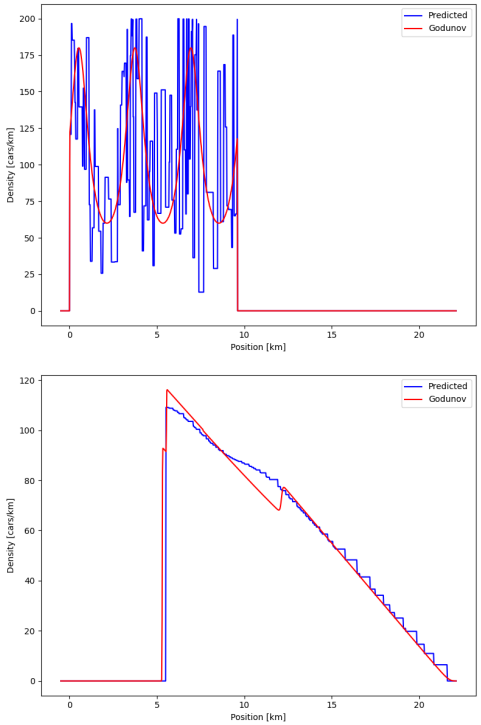

(a) $N = 1000$

Comparison of reconstructed and macroscopic densities
Top Initial densities
Bottom Final densities

Stop-and-go wave scenario

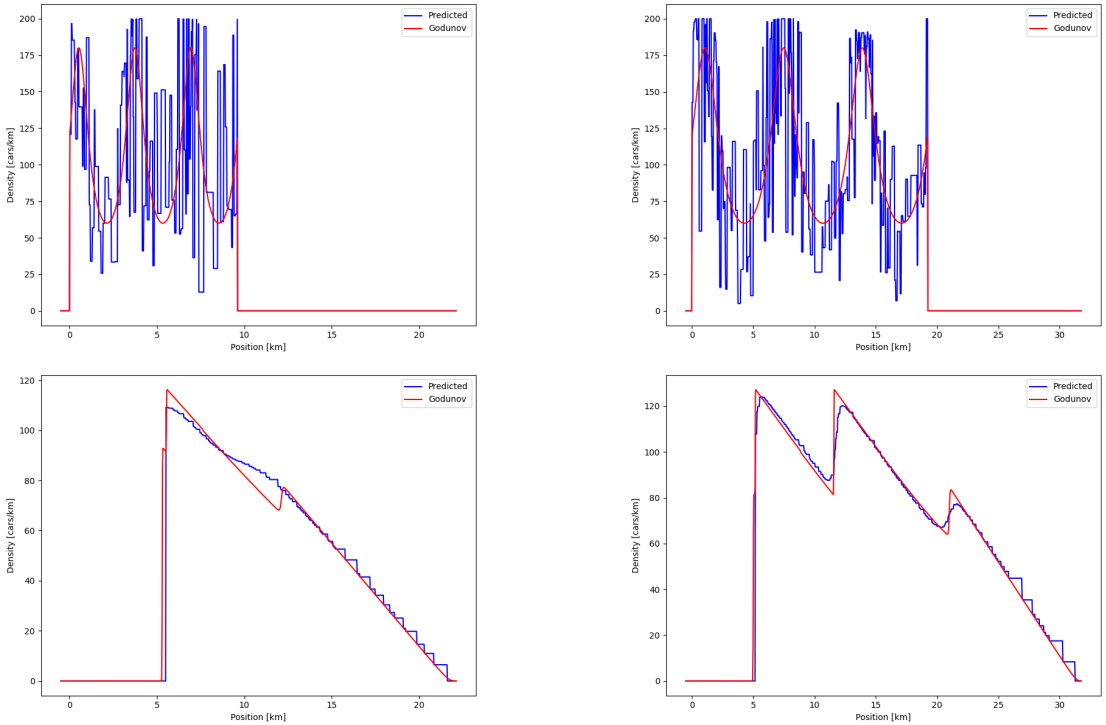

(a) $N = 1000$ (b) $N = 2000$

Comparison of reconstructed and macroscopic densities
Top Initial densities
Bottom Final densities

Stop-and-go wave scenario

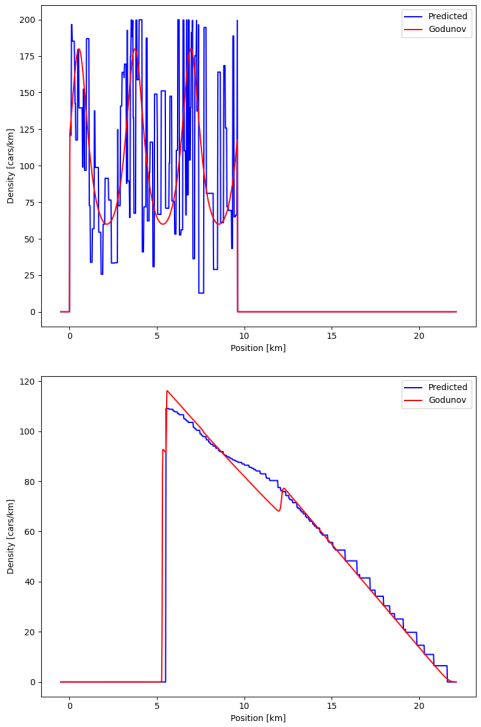

(a) $N = 1000$

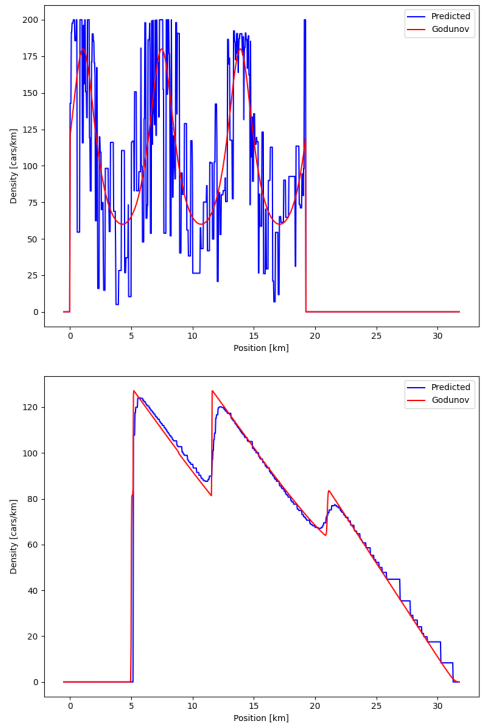

(b) $N = 2000$

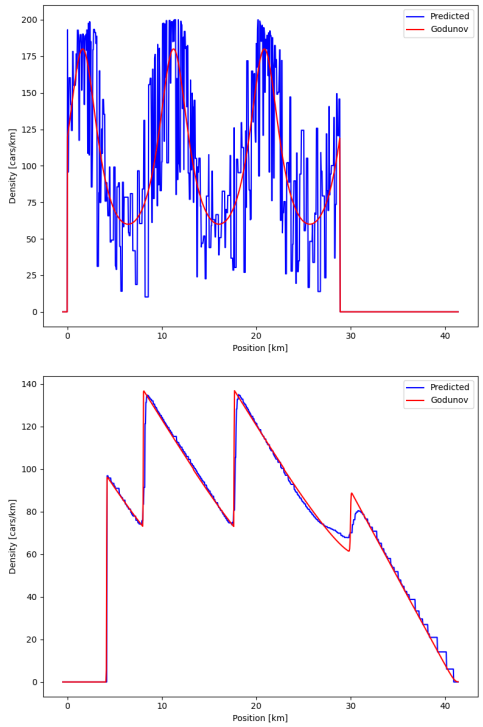

(c) $N = 3000$

Comparison of reconstructed and macroscopic densities
Top Initial densities
Bottom Final densities

Stop-and-go wave scenario

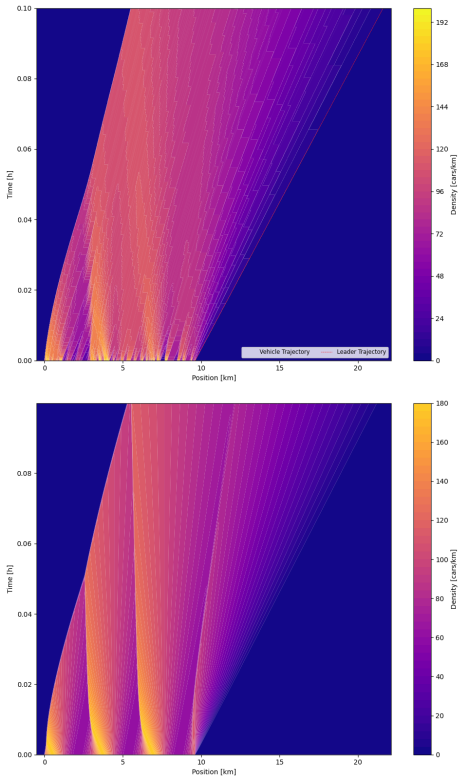

(a) $N = 1000$

Comparison of **reconstructed** and **macroscopic** densities
Top Reconstructed density from learning-based optimization
Bottom Macroscopic density from LWR PDE (Godunov scheme)

Stop-and-go wave scenario

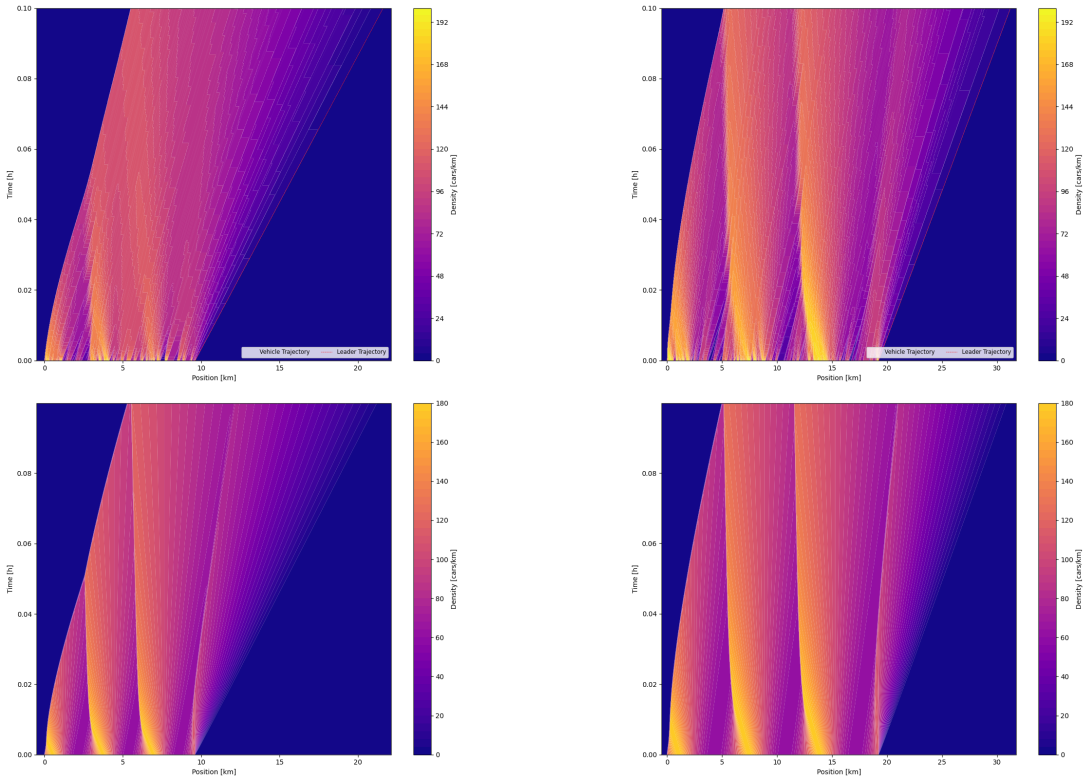

(a) $N = 1000$ (b) $N = 2000$

Comparison of **reconstructed** and **macroscopic** densities
Top Reconstructed density from learning-based optimization
Bottom Macroscopic density from LWR PDE (Godunov scheme)

Stop-and-go wave scenario

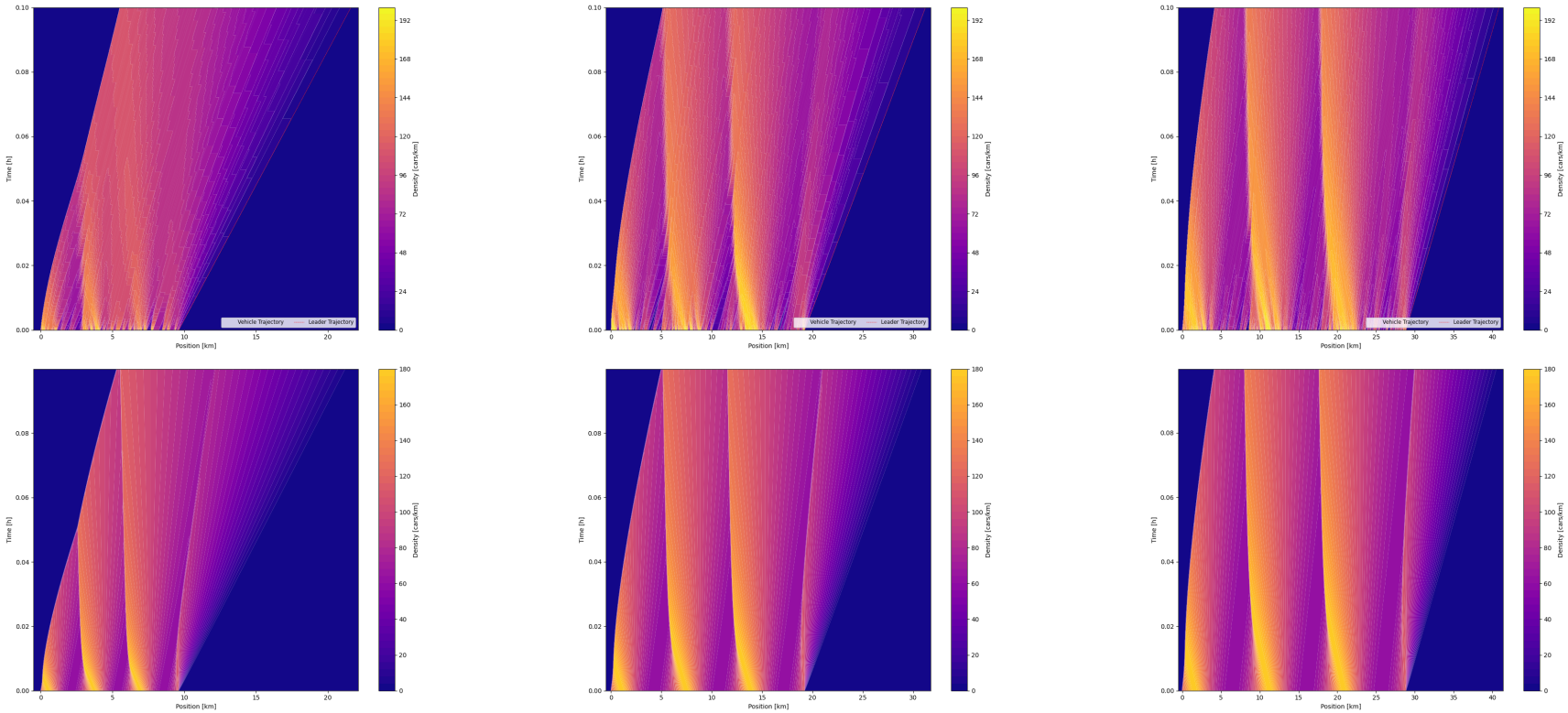

(a) $N = 1000$ (b) $N = 2000$ (c) $N = 3000$

Comparison of **reconstructed** and **macroscopic** densities
Top Reconstructed density from learning-based optimization
Bottom Macroscopic density from LWR PDE (Godunov scheme)

Table of Contents

Conclusion

Traffic State Reconstruction Approaches

- Model-Based Method
  ⇒ uses microscopic and macroscopic models
  ⇒ provides theoretical guarantees
  ⇒ struggles to capture real-world complexities
- Data-Driven Method
  ⇒ learns patterns directly from measurement data
  ⇒ derives system properties or predicts near-future states
  ⇒ requires extensive data for effectiveness
- Our Approach
  ⇒ combines models and data to address sparsity and improve realism
  ⇒ **Integrates physical priors with data observations**
  ⇒ achieves reliable traffic reconstruction with limited observations

Perspectives

- Conservation law with unilateral constraint[7] (toll gate)

$$\begin{cases} \text{LWR PDE (4) with} \\ f(\rho(t,0)) \leq q(t), \qquad t > 0. \end{cases} \tag{19}$$

- Conservation law with moving bottleneck[8] (slow vehicle)

$$\begin{cases} \text{LWR PDE (4) with} \\ f\left(\rho(t,y(t))\right) - \dot{y}(t)\rho(t,y(t)) \leq \frac{\alpha \rho_{\max}}{4 v_{\max}} \left(v_{\max} - \dot{y}(t)\right)^2, & t > 0, \\ \dot{y}(t) = \omega\left(\rho(t,y(t)_+)\right), & t > 0, \\ y(0) = y_0 \end{cases} \tag{20}$$

- Network with a junction[9] J and N incoming roads and M outgoing ones

$$\begin{cases} \partial_t \rho_l(t,x) + \partial_x\left(f(\rho_l(t,x))\right) = 0, & t > 0, \quad x \in I_l, \quad l = 1, \dots, N+M \\ \rho_l(0,x) = \rho_{0,l}(x), & x \in I_l = [a_l, b_l], \quad l = 1, \dots, N+M \end{cases} \tag{21}$$

$\Rightarrow \sum_{i=1}^{N} f\left(\rho_i(t,(b_i)_-)\right) = \sum_{j=N+1}^{N+M} f\left(\rho_j(t,(a_j)_+)\right)$ (Rankine Hugoniot)

$\Rightarrow \sum_{i=1}^{N} f\left(\rho_i(t,(b_i)_-)\right)$ is maximized with $f\left(\rho_j(\cdot,(a_j)_+)\right) = \sum_{i=1}^{N} a_{j,i} f\left(\rho_i(\cdot,(b_i)_-)\right)$

[7] **colombo˙well˙2007**.
[8] **liard˙entropic˙2020**.
[9] **coclite˙traffic˙2005**.

References I

Scheme of Model

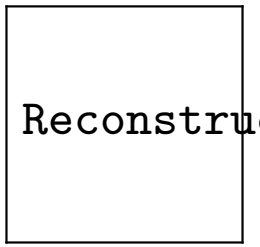

Traffic Flow Reconstruction Pipeline

Convergence of Model

- Weak solution of (4) is entropy admissible if it satisfies Kruzhkov entropy condition

$$\int_0^T \int_{\mathbb{R}} |u-k| \frac{\partial \phi}{\partial t} + \operatorname{sign}(u-k)(f(u)-f(k)) \frac{\partial \phi}{\partial x} dx dt \geq 0, \quad \forall k \in \mathbb{R} \tag{22}$$

Convergence of approximate density to solution of LWR

Under some assumptions, piecewise-constant density

$$\rho^N(t,x) = \sum_{i=0}^{n-1} \frac{\bar{\alpha}_i^N L}{N(x_{i+1}^N(t) - x_i^N(t))} \chi_{[x_i^N(t), x_{i+1}^N(t))}(x), \quad x \in \mathbb{R}, \quad t \in [0,T], \tag{23}$$

where $\bar{\alpha}_i^N \in \mathcal{A}_N$ is a solution to (13) converges to **unique entropy** solution ρ of

$$\begin{aligned} &\frac{\partial \rho}{\partial t}(t,x) + \frac{\partial f(\rho)}{\partial x}(t,x) = 0, \quad x \in \mathbb{R}, \quad t \in [0,T], \\ &\rho(0,x) = \rho_0(x), \quad x \in \mathbb{R}. \end{aligned} \tag{24}$$

- Typically, we impose a condition of type

$$\max_{i=0,\dots,n-1} \alpha_i^N = o(N). \tag{25}$$

$\Rightarrow$ ensures controlled growth of α_N